

Article

Links between Ikaite Morphology, Recrystallised Ikaite Petrography and Glendonite Pseudomorphs Determined from Polar and Deep-Sea Ikaite

Bo Pagh Schultz ^{1,*}, Jennifer Huggett ², Clemens V. Ullmann ³, Heidemarie Kassens ⁴ and Martin Kölling ⁵

¹ Fur Museum, Museum Salling, Nederby 28, 7884 Fur, Denmark

² The Natural History Museum, Cromwell Road, London SW7 5BD, UK; jmhuggett@icloud.com

³ Camborne School of Mines, University of Exeter, Penryn Campus, Penryn TR10 9FE, UK; c.ullmann@exeter.ac.uk

⁴ GEOMAR Helmholtz Centre for Ocean Research Kiel, Wischhofstraße 1-3, 24148 Kiel, Germany

⁵ MARUM Center for Marine Environmental Sciences, University of Bremen, Leobener Str. 8, 28359 Bremen, Germany

* Correspondence: bosc@museumsalling.dk

Abstract: Petrography of recrystallised ikaite from Ocean Drilling Program material has been presented previously from Nankai Trough and Congo (ex-Zaire) deep-sea fan. This paper expands on the Nankai Trough ikaite observations, drawing on evidence from Laptev Sea, South Georgia, Okhotsk Sea, and coastal lagoon Point Barrow. However, even though many ikaite and glendonite sites occur at high latitudes, it cannot be that ikaite forms exclusively in polar environments, as demonstrated by the occurrences in the low latitude low temperature deep sea sediments offshore Gulf of Guinea (Angola Congo) and mid-latitude deep-sea trenches offshore Japan. Recrystallised ikaite occurs as mm large, zoned calcite crystals in all samples, along with secondary phases of calcite. Our data set is unique in that the origin, storage, and recrystallisation process of natural formed ikaite is recorded in detail and confirms that glendonite petrographic characteristics are a consequence of the structure and chemistry of recrystallising ikaite and not the physical or geochemical environment. The transformation of man-made ikaite to calcite as recorded in laboratory studies, is a process very similar to the one we have observed for natural ikaite. Most significant is that there is variation in the order of the calcite types within a single sample, leading to the conclusion that the variation is a consequence of impurities and geochemical variability in the ikaite, not the external environment. Morphological observations reveal similarities in ikaite and glendonite, this and the similarity in internal textures in glendonite and recrystallised ikaite confirms that glendonite may be used as an indicator of past presence of ikaite.

Keywords: ikaite morphology; recrystallised ikaite petrography; links to glendonite

Citation: Schultz, B.P.; Huggett, J.; Ullmann, C.V.; Kassens, H.; Kölling, M. Links between Ikaite Morphology, Recrystallised Ikaite Petrography and Glendonite Pseudomorphs Determined from Polar and Deep-Sea Ikaite. *Minerals* **2023**, *13*, 841. <https://doi.org/10.3390/min13070841>

Academic Editors: Gabrielle J. Stockmann and Juan Diego Rodríguez-Blanco

Received: 16 May 2023

Revised: 14 June 2023

Accepted: 15 June 2023

Published: 22 June 2023



Copyright: © 2023 by the authors. Licensee MDPI, Basel, Switzerland. This article is an open access article distributed under the terms and conditions of the Creative Commons Attribution (CC BY) license (<https://creativecommons.org/licenses/by/4.0/>).

1. Introduction

This paper is dedicated to the marine geological institutes GEOMAR Helmholtz-Zentrum für Ozeanforschung, Kiel and MARUM—Zentrum für Marine Umweltwissenschaften der Universität Bremen in recognition of the profound importance their sampling and research has meant for this topic. Without samples shown in Figure 1 (Table 1), donated to our research this paper could never have been accomplished tying, the oddly formed pseudomorphs first named as pseudogaylussite and later known by other names now mostly referred to as glendonite. These pseudomorphs are usually formed of calcite, less often of opal or quartz. Since 1826 researchers have been baffled as to the nature of the pseudomorphs' parent mineral [1]. Historical and morphological aspects of glendonite have been described previously by the author and many other colleagues [1,2]. Details to

petrology evaluated repeatedly in the years 1836 to present [3–7]. Crystallography presenting a similar line of evaluations from the crystals were known to science, ranging from 1836 to present [8–12]. The link between glendonite and ikaite ($\text{CaCO}_3 \cdot 6\text{H}_2\text{O}$) first emerged when collected ikaite was found to recrystallise to a slush of calcite presented in 1982 to present [13–15]. However, the lack of stability of ikaite removed from where it formed to somewhere where it could be analysed, made further research a challenge. Most ikaite occurs at high latitudes, and most glendonites occur in sediments interpreted as having been deposited in low temperature environments [2,16].

In marine settings the mineral ikaite occurs in organic rich anoxic sediments where alkalinity is high and calcite precipitation inhibited. Ikaite forms yellow-orange monoclinic crystals with distinct prismatic faces, but due to the metastability the ikaite rapidly recrystallises, even when kept in a freezer. X-ray diffractometry of frozen crystals has confirmed that they are ikaite as shown in 1983 [17] and 2022 [18] but the metastability has so far precluded optical goniometric examination. Glendonite typically has more than one generation of calcite with distinct textures. The first to precipitate is prismatic zoned crystals <1mm long, which directly replace ikaite (type 1 calcite). These crystals typically have rounded overgrowths. Secondly, spherulitic calcite (type 2 calcite) may precipitate on the prisms, and finally calcite spar (type 3 calcite) partially or fully cements any remaining voids [19,20], both describing the most common petrographic fabric of type 1 and type 3 calcite as guttulatic. Rarely pseudomorphs are formed of quartz, or opal rather than calcite.

Since Erwin Suess retrieved an euhedral ikaite crystal from Bransfield Strait in 1982, there has been a growing acceptance that glendonite is a pseudomorph after the metastable ikaite. The similarity of the macroscopic morphology of ikaite to that of glendonite and the guttulatic microstructure of recrystallised marine ikaite also found in glendonite is convincing petrographic evidence that ikaite is the precursor to glendonite [7,19,21].

Sea of Okhotsk material consists of both glendonites and ikaite retrieved and published in 2004 [7]; see their Figure 2, F1, F2 and G. The material holds a special interest as sample G, the ikaite, later recrystallised in the GEOMAR facility and was provided for this study by Professor Jens Greinert of GEOMAR. In addition, included in this study are GEOMAR samples retrieved from the Laptev Sea in 1987 by Dr. Heidemarie Kassens [22] from 1995. These ikaite samples remained stable when kept at -18°C in the GEOMAR facility. The Nankai Trough samples were retrieved in 2012 by Martin Kölling and were stored at MARUM at -18°C . Yet, when examined in 2020 they had nearly fully recrystallised. This difference between the Laptev and Nankai samples is believed to be a consequence of the time spent logging and describing them, plus the rate of heating and presence of impurities by [18] in 2022. Hence, the cold storage may only have slowed down rather than prevented the process of recrystallisation.

The South Georgia sample was retrieved in 2017 by Gerhard Bohrmann from the Anakaov Trough and has undergone slow recrystallisation from within, as with the Laptev sample.

The pseudomorphs resulting from these observed recrystallisation processes, plus those recorded in 1987 for Point Barrow all have textures strikingly similar to those earlier described [19,23,24].

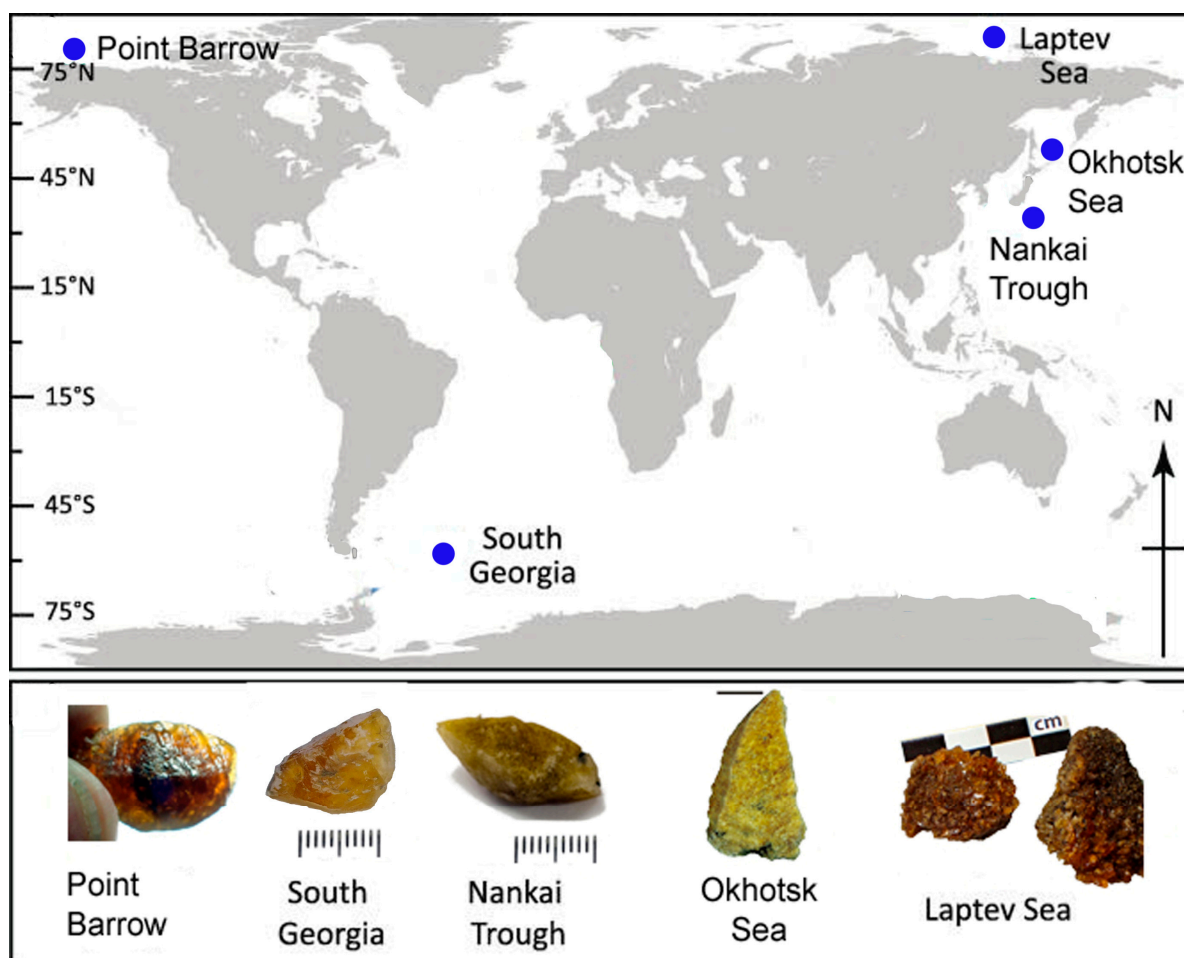


Figure 1. Ikaite sites and samples. Figure after [18]. Photo of Point Barrow was taken by G.L. Kennedy [2]. Illustration Okhotsk Sea is shown with permission from Marine Geology [7]. Where no other indication is listed in this article all images are taken by the author.

Table 1. Listing of the initial cruise reports or the published articles containing extensive data on settings and geochemistry. Some data for samples from Okhotsk Sea and Isatkoak have been previously published. Samples from South Georgia, Nankai Trough and Laptev Sea have previously only been shown as images in cruise reports.

Ikaite Location		Lat/Long	Water Depth (m)	Depth below S-W Interface (m)	Site Tag	Sample Tag	Reference
Utqiagvik Alaska	Isatkoak Lagoon	71°23'20" N 156°28'45" W	3	Shallow			[23]
Sea of Okhotsk	Offshore Sakhalin	05°59.6' S, 09°56.6' E	380	2	Site lv27-3-3 n-Sakhalin 5		[7]
South Georgia	Anakaov Trough W	54°23.2' S, 37°30.8' W	359	5.7	Cruise M134 S Georgia	GeoB-Number: 22049-3	[25]
Nankai Trough	Japan Trench	31°50' N, 133°51' E	6900	4.3	Core GeoB16423-1	GeoB 16427-1-460	[26]
Laptev Sea	Siberia	78°04.5' N, 133°35.9' E	204	2.32 to 2.38	ARCTIC'93 exped., Core PS2460-4	IKAITE PM 9499-2	[22]

2. Methods

2.1. Scanning Electron Microscopy

A Tescan Mira3 High Resolution Schottky Field Emission (FEG-SEM) fitted with both standard and in-lens secondary electron, as well as back-scattered electron detectors at Lund University was used to observe ikaite transformation in order to further constrain the nature of the transformation. Uncoated samples of ikaite, taken from the freezer, were

mounted on stubs at ambient temperature (c. 21 °C) and were run in the SEM under low vacuum mode at a pressure of 60 Pa, with no additional temperature regulation. The acceleration voltage was set to 15 kV and the working distance varied between 5 and 15 mm.

2.2. Inductively Coupled Plasma Optical Emission Spectrometry (ICP-OES)

Minor element analyses were undertaken on powdered, bulk-dried, transformed ikaite, now calcite, in Table 2 using an Agilent 5110 VDV ICP-OES at the Camborne School of Mines, University of Exeter, following the method detailed [27]. The minor element data are expressed as ratios to Ca and calibrated using certified single-element standards mixed to match the chemical composition of the analysed samples. Precision and accuracy of the analyses were measured and controlled by interspersing multiple measurements of international reference materials, JLS-1 and AK, and quality control solution (BCQ2).

2.3. Introduction to Petrography Approaches

Macro- and microscopic textures of ikaite and ikaite undergoing recrystallisation that illustrate the transformation to pseudomorphs are shown in Figure 2. Due to the notorious instability of ikaite when removed from the environment in which they precipitated, it has been hard to document the transformation process in detail. Figure 2 shows rapidly captured images, pre-recrystallisation of distinct ikaite crystal faces and overall morphology (Figure 2a), also seen in glendonite (Figure 2b). Crystal faces are as described in early papers, e.g., [9], though we now contribute the first systematic approach to the correlation between single ikaite crystals and general glendonite morphologies and petrography.

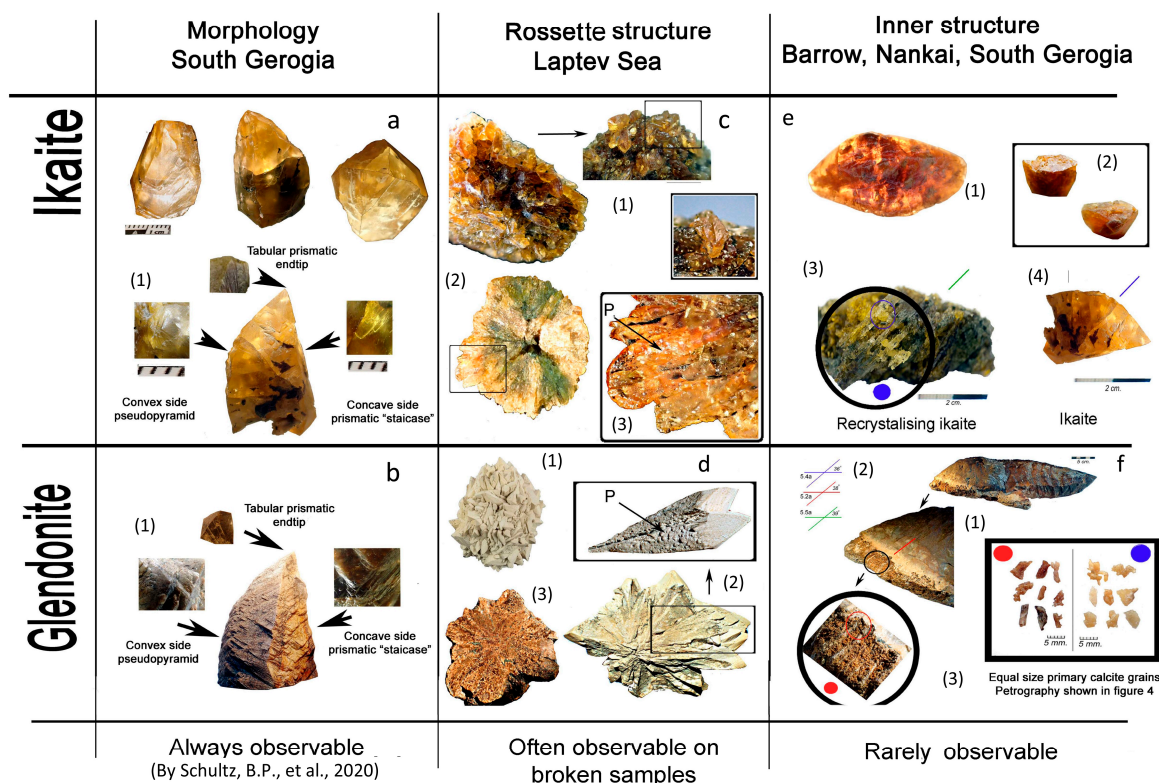


Figure 2. Macroscopic and petrographic results. (a) South Georgia ikaite (same sample as in Figure 1); (b1) Danish glendonite with similar morphology to the South Georgia ikaite [28]. (c) Detail from the Laptev sample shown in Figure 1, showing that (c1) are minute incomplete crystals; (c2) shows the inner rosette structure of (c1). (c3). show enlarged detail of minute reflection interpreted as pseudo pyramids, marked as (P) as in (d2). (d1–d3) Rosette glendonite nodules from a Cretaceous Russian Taymyr sample. Image in box shows detail of pseudo pyramids (P) in (d2). Sample (d3) is a fully cemented Permian glendonite from New South Wale in Australia, site Wallaby canyon. (e1–e4)

Inner structures and impurities from Barrow samples (same samples as Figure 1). (e2) Linear distribution of primary calcite at the onset of recrystallisation, Nankai ikaite (photo by Volker Diekamp GeoB16423_1_VD22238); (e2) has brittle cracks, not seen in Nankai (e3) and South Georgia (e4) where the structures appear to be related to inner structure of the ikaite crystal. (f) shows rarely observed petrographic features that are strikingly similar in glendonite and ikaite. (f1) Glendonite from Fur formation where the tip has a weathered surface, exposing the inner structure also show in ikaite in (f2). Sample (e3) South Georgia ikaite showing possible cleavage planes. (f3) The coloured dots indicate sampling places from (e3,f1). Whereby showing individual primary calcite grains from Danish glendonite and recrystallised Nankai ikaite are very similar in shape and size, though the Danish pseudomorph is much larger in overall size than Nankai.

3. Results

3.1. Macroscopic Morphology and Petrography

The distinctive internal texture of glendonite, with chemically zoned mm-sized calcite crystals in microcrystalline matrix by [19,24,29], is also present in recrystallised ikaite [20]. The texture is characterised by pseudo-hexagonal or spherical low-Mg cores, with an ellipsoidal overgrowth, and secondary high-Mg sparry or micritic cement. In some instances, a spherulitic form of calcite has precipitated prior to the micrite. Eva Scheller named this texture “guttulatic”, after the Greek work for little drop and shows many examples in [20,30]. The process shown in Figure 3 and petrological details in Figure 4.

Ikaite ➤ Recrystalising ➤ Calcite ➤ Guttulatic petrology

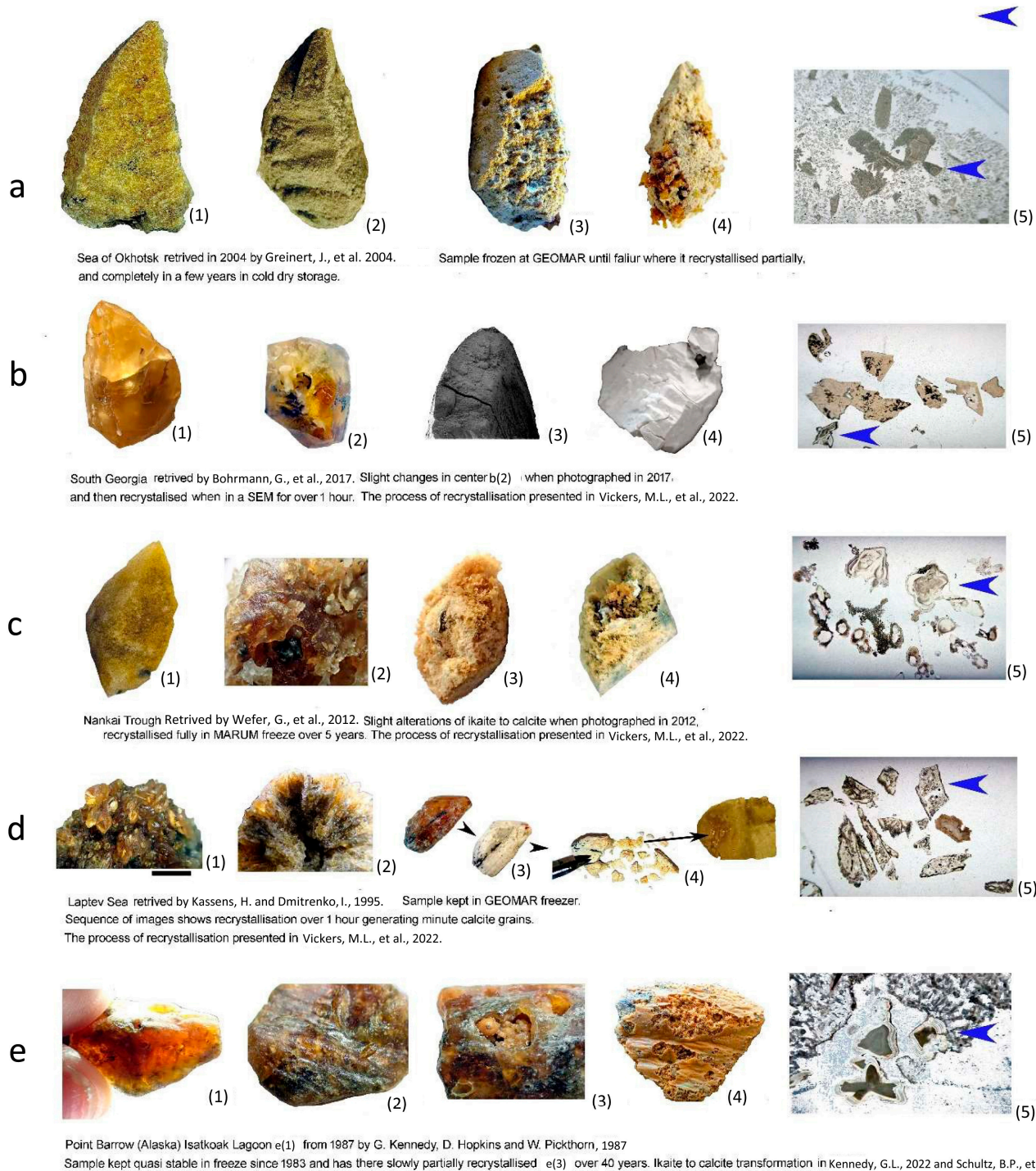


Figure 3. All samples have recrystallised in air at normal pressure with nothing present other than the original components of the ikaite, as ikaite transformed to calcite [18]. (a1) Sea of Okhotsk ikaite (reproduced from Figure 2 in [7]), (a2) Same sample recrystallised when the Geomar freezer broke down. (a3) Sample disintegrating to form a porous calcite matrix under a thin crust. (a4) Sample after further disintegration, exposing guttulatic grains in calcite mush. (a5) Plane polarised light thin section image. (b1) South Georgia sample image take just before being imaged in a SEM [25]. (b2) Bottom view of same sample shows that inner recrystallisation has started [18]. (b3) SEM image of transforming ikaite. (b4) samples recrystallised after being in an SEM for 1 h. (b5) Plane polarised light thin section image. (c1) Nankai Trough ikaite crystal, photo (by V. Diekamp,

GeoB16425_1_VD22270) [26]. (c2) Nankai ikaite recrystallizing [18]. (c3). Sample (c1) after 6 years at minus 18 is recrystallised. A process that probably began during sample retrieval and has continued slowly due to the low temperature. (c4) Same sample, fully recrystallised. (c5) thin section image of Nankai recrystallised ikaite. (d1) Laptev Sea ikaite, comprising mm-sized bright yellow/orange semi-transparent ikaite from Laptev [22]. (d2) Inner structure. (d3) Inner structure fragments after 2 h at room temperature, recrystallised into an off-white mush of calcite [18]. (d4) same sample, disintegrated into micritic calcite crystals, [31], (d5) thin section image of Laptev recrystallised ikaite. (e1) Point Barrow Isatkoak Lagoon crystals verified to be ikaite [23,24], (e2) Partial recrystallisation seen as whitish impurities [2]. (e3) Shows natural recrystallisation occurring in frozen dry storage over a duration of 40 years. (e4) Fully recrystallised to calcite in [24]. (e5) Plane polarised light thin section image (Isatkoak photographed by G. Kennedy). Thin sections imaged in (b5,c5,d5) are shown in greater detail in Figure 4.

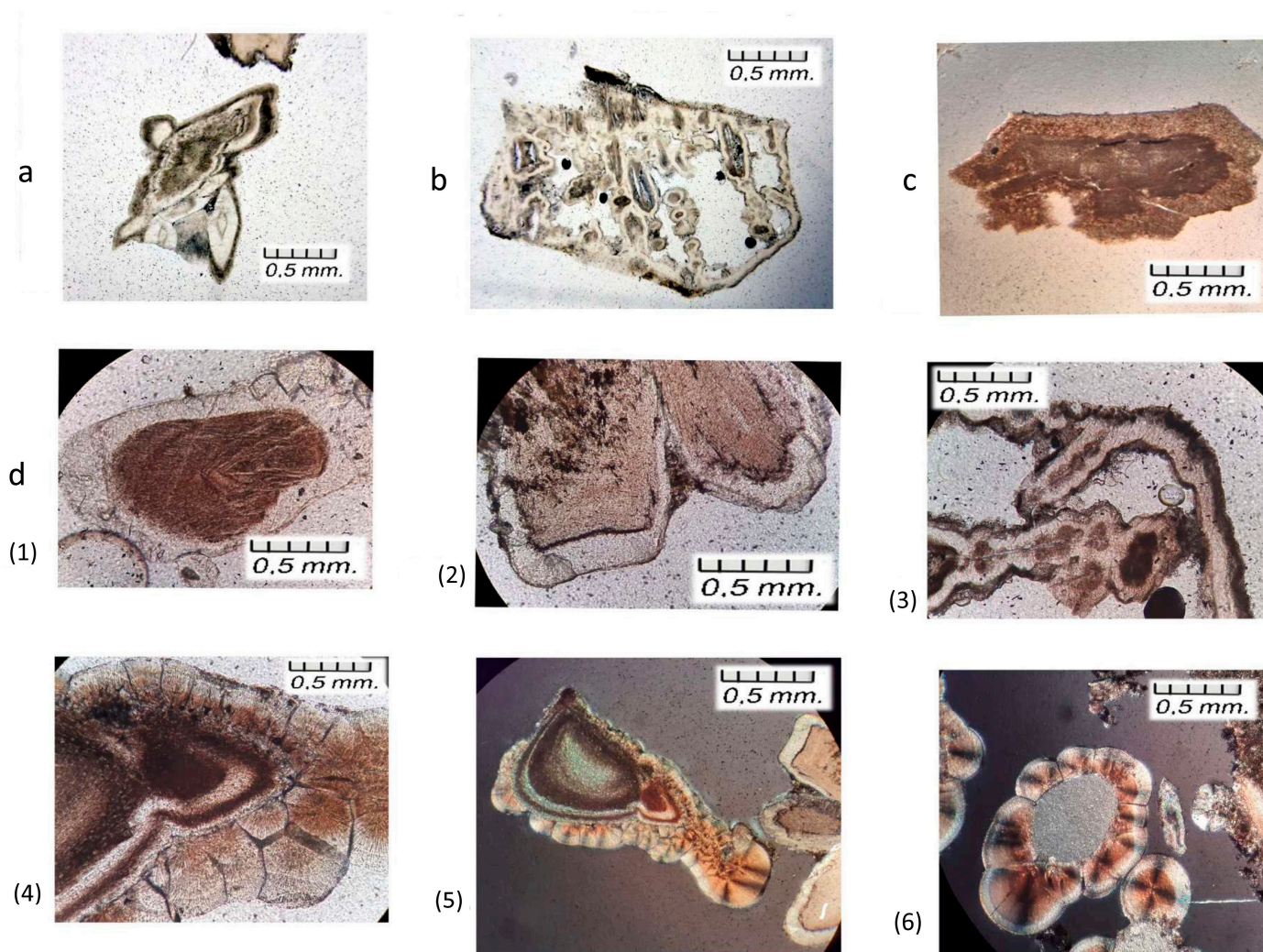


Figure 4. Optical microscopy of samples from South Georgia, Laptev Sea and Nankai Trough. Images are of the same samples shown in Figure 3. All samples recrystallised in storage, excluded from a “normal” environment, hence variations are due only to the nature of the ikaite. Plane polarised optical microscope images of samples in Figures 1 and 2. Guttulatic structure is clearly visible in all images, though with morphological variations which may indicate variations in the recrystallisation process. (a) South Georgia sample showing guttulatic microstructure. (b) Laptev Sea matrix and rim. (c) Laptev Sea sample, small crystal with two growth stages, both guttulatic. (d1) Nankai Trough samples 602 and Nankai 94 (this paper Figure 3(c1)) matrix samples are loose grains sampled from crumbling matrix. (d2) guttulatic morphology in primary core and overgrowth by non-guttulatic cement. (d3) Guttulatic grains and rim cement. (d4). Variation in guttulatic intensity and botryoidal calcite that has overgrown guttulatic grain. (d5,d6) Images taken under polarised light,

showing two examples of a grain with non-guttulatic calcite at the core, overgrown by guttulatic calcite, followed by botryoidal calcite.

3.2. Geochemical Variations between the Petrographic Types

Geochemical analyses of the host sediments and ikaite/glendonite have been previously obtained (e.g., [6,7,18–21,24,29–33]). Here we provide greater detail of the process recognized whereby ikaite rapidly recrystallises into distinct calcite types without addition of porewater ($\text{CaCO}_3 \cdot 6\text{H}_2\text{O} \rightarrow \text{CaCO}_3 + 6\text{H}_2\text{O}$) [7,18,20,25,26], See Table 2.

3.3. Crystal Morphology and Structure

As yet, it has not been possible to determine the true symmetry of ikaite (monoclinic m2 class?) due to its instability in laboratory conditions. In monoclinic m2 class the primary cleavage defines the Miller 010. To date we have only succeeded in measuring ikaite from one South Georgia sample and four Point Barrow samples. This data shows that there is a cleavage plane perpendicular to the elongation of the crystal, and in the South Georgia sample there is what appears to be a cleavage at a 45° angle to the elongation. The monoclinic affinities are observable in ikaite and glendonite. The affinity being that in samples such as those shown in Figure 2(e1,f1), the tips bend off in opposite directions, so that a bladed crystal in its elongated growth direction will present a set of concave and convex edges ordered diametrically opposite.

3.4. Calcite Phases Shown in Figure 4 Summarised

All the recrystallised ikaite samples have guttulatic textures, similar to the type 1 cement [19]. This can be subdivided by variations in type 1(I) and 1(II) calcite as discussed by others in [18,32]. Late-stage sparry calcite is identified as type 3 in [19] and type III in [28], respectively. Guttulatic calcite is sometimes overgrown by Type 2 botryoidal calcite [24,28], though this mode of growth is not always present, e.g., Figure 4 suggested that impurities may be responsible for the type 2 growth form, as noted previously [18].

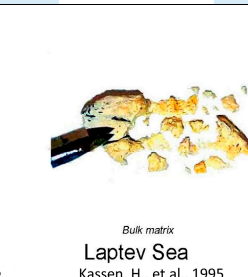
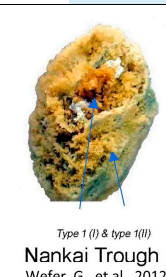
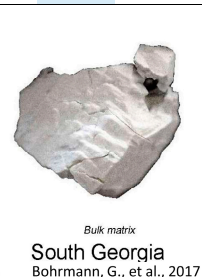
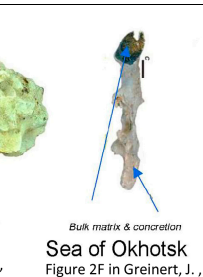
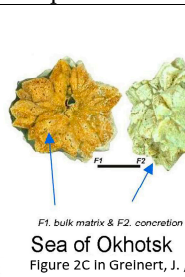
3.5. Geochemical Distribution in the Petrographic Types

The geochemistry of both host sediment and ikaite have been previously described by [7,25,26]. To this we add new chemical data (Table 2) demonstrating that even when CaCO_3 is 100 %, there are minor and trace elements present. Even in a closed system, i.e., no porewater present, it is these elements that control the rate and temperature of ikaite decomposition ($\text{CaCO}_3 \cdot 6\text{H}_2\text{O} \rightarrow \text{CaCO}_3$) [18].

Table 2. Single grains representing the sequence of ikaite recrystallisation events that have been analysed using optical emission spectrometry. The samples are the same as in Figures 1–3 [22,25,26], with the addition that Sea of Okhotsk samples [7] from the same site as those analysed for this paper are included for comparison. The results illustrate the difference in element ratios between calcite formed only from ikaite recrystallising (light blue) to calcite derived from ikaite recrystallising in water saturated sediment. Element ratios from individual calcite types are compared with fully cemented, and diagenetically altered samples (grey). Highlighted in light green is data for Nankai host sediment, a muddy marine turbidite, included to demonstrate likely porewater influence on the geochemistry of glendonite.

Sample	CaCO_3	Mg/Ca	Sr/Ca	Na/Ca	Mn/Ca	Fe/Ca	S/Ca	P/Ca	Al/Ca	Rb/Ca
	wt%	mmol/ mol	mmol/ mol	mmol/ mol	mmol/ mol	mmol/ mol	mmol/ mol	mmol/ mol	mmol/ mol	mmol/ mol
Sample in Figure 3(a4)—Sea of Okhotsk type 1, large orange calcite	100.00	17.89	1.12	7.61	0.00	0.05	0.33	0.60	0.10	LOD
Sample in Figure 3(a4)—Sea of Okhotsk type 2, yellow calcite	100.00	6.02	1.00	3.07	0.00	0.05	0.25	0.11	0.29	LOD
Sample in Figure 3(a4)—Sea of Okhotsk matrix, fine-grained white calcite powder	93.14	2.99	1.04	6.91	0.00	0.01	0.23	0.17	0.15	LOD

Sea of Okhotsk [7], their Figure 2C tracefossil burrow concretion	51.79	112.39	1.81	23.17	0.62	29.45	17.57	4.48	56.02	LOD
Sea of Okhotsk [7], their Figure 2C tracefossil burrow calcite matrix	85.86	68.82	1.82	6.57	0.27	5.29	8.48	4.45	2.72	LOD
Sea of Okhotsk [7], their Figure 2F glendonite concretion	65.65	69.83	1.42	23.90	5.79	41.44	3.73	12.61	44.92	LOD
Sea of Okhotsk [7], their Figure 2F glendonite calcite matrix	100.00	99.40	1.71	6.52	0.09	0.37	1.04	5.87	0.57	LOD
Sample in Figure 3(b4)—South Georgia bulk calcite	93.06	0.46	1.22	1.11	0.01	0.06	1.56	0.26	0.17	LOD
Sample in Figure 3(c4)—Nankai Trough, sediment fragments as reference	49.74	60.21	0.76	119.49	0.33	27.06	30.21	0.47	32.63	0.11
Sample in Figure 3(c4)—Nankai Trough type 1, large orange calcite grains	100.00	25.36	0.84	11.20	0.01	0.12	11.96	0.31	0.39	LOD
Sample in Figure 3(c4)—Nankai Trough type 2, yellow calcite grains	91.84	4.10	1.28	23.26	0.01	0.31	6.99	0.11	0.73	LOD
Sample in Figure 3(d4)—Nankai Trough type3, fine grained calcite	91.60	1.44	1.40	25.03	0.01	0.21	7.69	0.05	0.51	LOD
Sample in Figure 3(d4)—Laptev Sea bulk calcite	91.10	2.37	0.60	4.47	0.08	1.15	0.79	0.36	1.31	LOD



LOD = Limit of Detection.

4. Discussion

4.1. Recrystallised Ikaite Calcite Types

We show that the Okhotsk Sea ikaite sample (their Figure 2G, our Figure 3(a2–a5)) recrystallised in a contaminant-free environment has distinctly different chemistry to the ikaite analysed [7] samples in Figure 2C,F. We show that the matrix is much closer to the element ratios of the crust than to those of uncontaminated ikaite. Figure 7 on page 141 [7] provides an excellent overview of the chemical changes occurring during diagenesis from nucleation of ikaite to recrystallisation.

Nankai and Laptev contaminant free ikaite recrystallised to calcite with a similar chemistry to the contaminant free Okhotsk Sea sample, which is consistent with the chemistry being controlled by the process not the environment. Mg and trace element concentrations vary between the calcite cement types, but not in a consistent way between samples (Table 2) [24,31,32].

Lately Whiticar demonstrated that Bransfield ikaite [33] might be confined to a specific geochemical zone that is the interval of hydrogenotrophic methanogenesis between the sulphate reduction zone and the deeper zone of methanogenesis. Whiticar in their Figure 7, in [33] show isotopic variation of O^{18} and C^{13} from the inner core to the outer rim of an ikaite, implying chemical and isotopic shifts during recrystallisation. The Bransfield ikaite has an isotopic composition that changes from the centre towards the rim, implying that the rim cement defines the shape of the ikaite and must have formed prior to wholesale dissolution of the ikaite, for the mesh of calcite grains contained within the structure, and later calcite spar to have cemented the structure without any infilling by sediment.

4.2. Petrographic Comparison of Ikaite and Fur Formation Glendonite

It is currently unclear whether glendonite pseudomorphs form through ikaite recrystallisation alone, or if there are interactions between ikaite and the sediment pore waters. All samples discussed here were recrystallised in controlled settings where the water lost during ikaite decomposition was retained as the only porewater present.

Information from Fur Formation glendonites, especially petrographic data [19], was selected for detailed comparisons with the artificially recrystallised ikaite. In Fur Formation ikaite, recrystallisation and subsequently secondary carbonate infill occurred at pH 5.5 to 8 [34–36]. The bottom water temperature has been estimated to $>5^{\circ}\text{C}$ based on δ_{47} presented in [37], while the diagenetic temperature was no higher than 38°C in [38,39]. Estimated water depth is 200–400 m (equal to 0.2 to 0.4 kilobar), based on trace fossils (ichnofacies), including bathyal zone Zoophycos in the Holmehus Clay and sublittoral Teichichnus in younger Fur Formation sediments representing a basin change presented [40,41]. Sea surface temperature (SST) obtained by Tex 86 to be 10°C higher during the PETM onset reaching up to $\sim 33^{\circ}\text{C}$. [42], flowed by a slow decent to post-PETM SST of $11\text{--}23^{\circ}\text{C}$). Other advantages of using the Fur Formation for comparison are the excellent preservation [39,43–46], and well-defined time frame [36,41]. Many other pseudomorph sites exist [19,20] but none with the pristine preservation of Fur formation pseudomorphs.

Fur Formation glendonites occur super-size, in up to 1.5 m wide clusters, in marine diatomite with interbedded tephra layers [28]. The size of the calcite crystals varies little and is unaffected by the overall size of the pseudomorph [19,30]. Crystals ~ 1 mm have been extracted from cm size recrystallised Nankai ikaite (Figure 2(f3)) and compared to grains retrieved from 1 m sized Fur Formation weathered glendonite (Figure 2f). Both have a guttulate structure. Similar grains have been observed by the first author for glendonite from Olenitsa, on the White Sea and in Sea of Okhotsk in this paper. Each and every petrographic detail that can be observed in Fur Formation glendonite (Figure 5) correlates with textures seen in recrystallised ikaite (Figure 5).

Several ikaite break down models have been presented in [20,29,47] and demonstrated that Amorphous Calcium Carbonate (ACC) played an important role during the ikaite to calcite transition, and it is suggested that carbonate and calcium ions change orientation during loss of structural water [48]. Both these mechanisms are consistent with the observation illustrated in Figure 2a,(e3) of a possible structural element rarely observed in the glendonite (Figure 2f) forming along inner structures preserved in the pseudomorph. Given that the sample in Figure 2a from South Georgia was retrieved from 359 m depth and that in Figure 2(e1) is from 6900 m depth in the Nankai Trough suggests that the shown recrystallised is inherited from the inner structure of ikaite, an observation not previously made of euhedral marine ikaite. The recrystallisation is faster in the Nankai samples due to the significant pressure change, and possibly due to impurities making the ikaite recrystallise more rapidly.

In addition, striking is that the primary calcite crystals have a constant size, regardless of ikaite or pseudomorph size, as shown in Figure 2(f3), and in other publications [1,19,20,24]. Such a widespread observation implies that the controlling factor in crystal size is micro- (geochemical or microstructural) rather than macro-environmental. The concurrence of petrological details between Danish glendonite and the recrystallised ikaite is consistent with ikaite recrystallisation to glendonite (Figure 5).

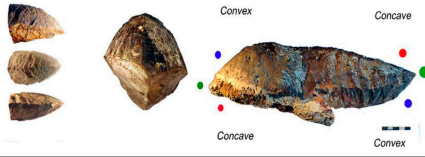
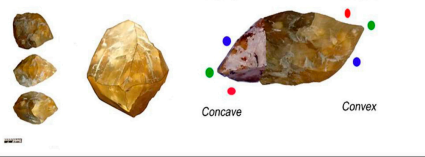
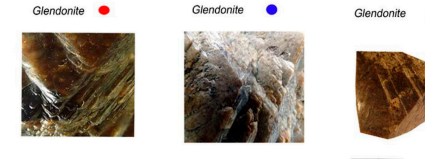


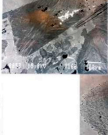



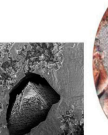
	Schultz, B.P., et al., 2020 Danish megasize glendonite	Bohrmann, G., et al., 2017 and Wefer, G., et al., 2012 Ikaite from South Georgia, Nankai Trough and recrystallised Nankai ikaite
Morphology Four sides to a crystal Two concave sides with prismatic faces Two convex sides with pyramid faces Prismatic tabular end tip		
Morphology of key features are same in both		
Primary mm large grains with guttulate structure - type 1(I) Primary mm large grains with dendritic structure - type 1(II) Secondary botryoidal cement - type 2	Type 1(I)  Type 1(II)  Type 2 	Type 1(I)  Type 1(II)  Type 2 

Figure 5. Guttulatic calcite grains (type 1) precipitate first; these are overgrown by type 1 II dendritic calcite [25,26,28]. The dendritic structure is a consequence of variation in the Mg concentration [49]. The botryoidal calcite phase (type 2) has overgrown types 1 and 1 II. This textural pattern only occurs as a result of ikaite recrystallisation, an observation not previously demonstrated. Individual crystals are frequently the same size, i.e., a few mm, despite the size of the pseudomorph. The SEM image is taken by Carl Alwmark of recrystallised ikaite type 1, and is the same grain as shown in a 2022 detailed description of this sample recrystallising [18].

4.3. Morphology and Cleavage

The morphology of typical glendonite has been known and described for a long time since 1884 [1,2,9,10,12], with excellent illustrations, where all the morphological details can be observed. If glendonite morphology had adhered to a standard monoclinic symmetry such as that of gaylussite or lenticular gypsum the early researchers would have been able to correctly identify the symmetry class. Ito attempted to identify the Miller axes for samples from Shiowakka Springs [6], yet the presented illustrations do not enable us to draw any conclusions concerning these axes for the South Georgia and Barrow samples because they are very different in shape. However, morphological similarities between ikaite and glendonites (Figure 2a,b), including the crystal curvature, are observed. It has been demonstrated that what at first appears to be a mirror plane along the crystal elongation [46], is in fact distorted, as the tips are twisted and the pinacoid prismatic faces are not in perfect symmetry. This observation is also applicable to the South Georgia sample.

The structure is more complex than normal monoclinic M2 class, as it represents an order of twinning. The appearance and crystal faces do not concur with swallowtail twins of monoclinic M2 class selenite, or selenite cleavage. Based on Figure 2, morphological observations (Figure 2a,b) and possible cleavage/inner structure (Figure 2e,f), we can only suggest a symmetry of the “albite twinning law”, with a multiple repetition of parallel polysynthetic twins. As with monoclinic feldspars, glendonite shows repetitions of prismatic faces. Yet, the glendonite also has curved crystals, often referred to as monoclinic affinity—that suggests a more complex explanation than just Albite twinning. Even though the morphology has been scrutinised by many gifted crystallographers [1] and the parent mineral being ikaite is well documented, this 200-year-old enigma of the true symmetry

of marine euhedral ikaite is still debated. We hope that showing the new details of internal structure and external morphology may inspire new theories.

4.4. Similarities between Glendonite and Ikaite Morphology

Measurement of glendonite from 46 sites indicates that all have a convex and concave side, where the concave side has a “staircase” of prismatic faces that appear to be pinacoid, and the convex faces display pseudo pyramidal structures in [46]. The pyramids slightly converge in rounded fan-like structures. Though our observation of ikaite only relates to a South Georgia sample and images from Nankai taken by Volker Diekamp (MARUM), it is evident that every single key feature suggested to define glendonite structure is present in the ikaite. The tip not being a point but a prismatic structure, is similar for both ikaite and glendonite. The most significant morphological observation is that surface structures observed on glendonite have been observed in exactly the same location and have the same appearance on the South Georgia ikaite. This is entirely consistent with glendonite being a replacement of ikaite and not some other form of sedimentary calcite, such as Cone in Cone.

5. Conclusions

Marine sediment-formed euhedral ikaite is now unequivocally identified as the parent mineral to glendonite, in modern as well as ancient marine glendonite-bearing settings. Guttulatic microstructure as a key identifier of recrystallised ikaite, is also present in glendonite. The mineral ikaite occurs in a very broad range of environments [1], whereas glendonite is restricted to sediment with a geochemical environment consistent with ikaite precipitation [35]. Other than when encountered in deep-sea landslides, glendonite can be considered a proxy for polar environments or short-lived cold intervals as demonstrated for the Fur Formation [32]. The symmetry of glendonite is not fully resolved, but the petrographic textures universally observed allow confident identification of these pseudomorphs (Figure 5). Demonstrated is the wide range of glendonite morphologies and the structures and petrology that they all have in common, and that we now are able to attribute that to ikaite as well [1,28]. Variations in morphology and textures may be linked to variation in Mg and organic impurities, rather than variations in the geochemical setting. Unequivocally linking glendonite to ikaite provides an improved opportunity to connect a larger range of glendonite morphologies to ikaite nucleation.

Author Contributions: B.P.S., writing—original draft; J.H., writing—review and editing; C.V.U., formula analysis; H.K., M.K. validation. All authors have read and agreed to the published version of the manuscript.

Funding: This project received funding by the Danish Council for Independent Research, Agency for Culture and Palaces (project MFO20.2017-004).

Data Availability Statement: Not applicable.

Acknowledgments: Our utmost gratitude to GEOMAR and MARUM staff for support and samples making this a unique paper to present. Special thanks to Erwin Suess, Jörg Thieden, Robert Spielhagen and Gerold Wefer paper. A special thanks must go to providers of exclusive samples, Jens Greinert, GEOMAR, and Gerhard Bohrmann, MARUM. Thanks to Alex Wülbers for ikaite transport and Volker Diekamp for images, along with good advice from Matthias Zabel from MARUM. Thanks to Carl Alwmark from the University of Lund for generating SEM images and Madeline Vickers for making the project manageable. A special thanks to co-author, Jennifer Huggett in particular for tireless effort of making this paper into a language quality much beyond the first author's ability to express, by which it is with pride we can present these fine results to colleges. I also would extend my thanks to the MDPI Editor and reviewers for offering good advice.

Conflicts of Interest: The authors declare no conflict of interest.

References

- Schultz, B.P.; Thibault, N.; Huggett, J.M. The minerals ikaite and its pseudomorph glendonite: Historical perspective and legacies of Douglas Shearman and Alec K. Smith. *Proc. Geol. Assoc.* **2022**, *133*, 176–192. <https://doi.org/10.1016/j.pgeola.2022.02.003>.
- Kennedy, G.L. Glendonites: Enigmatic mineral pseudomorphs and their ephemeral precursor. *Rocks Miner.* **2022**, *97*, 496–508. <https://doi.org/10.1080/00357529.2022.2087146>
- MacNair, P. *On pseudogaylussite dredged from the Clyde at Cardross and other recent additions to the Mineral Collections in the Kelvingrove Museum*. Proceedings of the Royal Philosophical Society of Glasgow: Glasgow, UK, 1904; 35, 250–262.
- Van Baren, J. *Bijdrage tot de kennis van pseudogaylussiet*. Mededelingen Geologisch Instituut Landbouw Hogeschool Wageningen: Wageningen, Netherlands, 1926; 10 pp. 1–24.
- Blum, J.R. *Die pseudomorphosen des mineralreichs*, E. Schweizerbat'che Verlagshandlung: Stuttgart, Germany 1843, pp. 13–17.
- Ito, T. Factors controlling the transformation of natural ikaite from Shiowakka, Japan. *Geochem. J.* **1998**, *32*, 267–273.
- Greiner, J.; Derkachev, A. Glendonites and methane-derived Mg-calcites in the Sea of Okhotsk, Eastern Siberia: Implications of a venting-related ikaite/glendonite formation. *Mar. Geol.* **2004**, *204*, 129–144, DOI: [https://doi.org/10.1016/S0025-3227\(03\)00354-2](https://doi.org/10.1016/S0025-3227(03)00354-2)
- KGUS Publishing, *Geologe Geologie Beruf Mineralogie Oryktognosie Mineralogen: Mineralien Naturwissenschaftler Naturwissenschaft Evoluti*, Independently published, 2020.
- Dana, E.S. A crystallographic study of the thynolite of Lake Lahontan. *U.S. Geological Survey Bulletin*, **1884**, *12*, 429–450.
- van Calker, F.J.P. XXIX. Beitrag zur Kenntniss des Pseudogaylussit und über dessen Vorkommen in Holland. *Z. Krist. Mineral. Geol.* **1897**, *28*, 556–572.
- Hintze, C. *Nitrate, Jodate, Karbonate, Selenite, Tellurite, Manganite, Plumbate, Handbuch der Mineralogie, Veit & Comp*; Der Verlag Walter de Gruyter & Co.: Berlin, Germany, 1915; pp. 2790–2802; 3650p.
- Goldschmidt, V.M. *Entwicklung d. Krystallformen II, Taf VIII & IX: Zeitschrift für Krystallographie und Mineralogie 28 bd*, Walter de Gruyter: Berlin, Germany, 1923.
- Suess, E.; Balzer, W.; Hesse, K.-F.; Muller, P. J.; Ungerer, C. A.; Wefer, G. 1982. Calcium carbonate hexahydrate from organic-rich sediments of the Antarctic shelf: Precursors of glendonites. *Sci.* **1982**, *216*, 1128–1131. <https://doi.org/10.1126/science.216.4550.1128>.
- Stein, C.; Smith, A. Authigenic carbonate nodules in the Nankai Trough, Site Initial reports of the deep sea drilling project. *Init. Repts. DSDP.* **1985**, *77*, 659–668.
- Jansen, J.; Woensdregt, C.; Kooistra, M.; Van Der Gaast, S. Ikaite pseudomorphs in the Zaire deep-sea fan: An intermediate between calcite and porous calcite. *Geol.* **1987**, *15*, 245–248.
- Rogov, M.; Ershova, V.; Gaina, C.; Vereshchagin, O.; Vasileva, K.; Mikhailova, K.; Krylov, A. Glendonites throughout the Phanerozoic. *Earth-Sci. Rev.* **2023**, *241*, 104430. <https://doi.org/10.1016/j.earscirev.2023.104430>.
- Hesse, K.F.; Küppers, H. Refinement of the structure of ikaite, $\text{CaCO}_3 \cdot 6 \text{H}_2\text{O}$. *Z. Krist.* **1983**, *163*, 227–231.
- Vickers, M.L.; Vickers, M.; Rickaby, R.E.; Wu, H.; Bernasconi, S.M.; Ullmann, C.V.; Bohrmann, G.; Spielhagen, R.F.; Kassens, H.; Schultz, B.P.; et al. The ikaite to calcite transformation: Implications for palaeoclimate studies. *Geochim. Cosmochim. Acta* **2022**, *334*, 201–216. <https://doi.org/10.1016/j.gca.2022.08.001>.
- Huggett, J.M.; Schultz, B.P.; Shearman, D.J.; Smith, A.J. The petrology of ikaite pseudomorphs and their diagenesis, *Proc. Geol. Assoc.* **2005**, *116*, 207–220. [https://doi.org/10.1016/S0016-7878\(05\)80042-2](https://doi.org/10.1016/S0016-7878(05)80042-2).
- Scheller, E.L.; Grotzinger, J.; Ingalls, M. Gutttalite calcite: A carbonate microtexture that reveals frigid formation conditions. *Geol.* **2022**, *50*, 48–53. <https://doi.org/10.1130/g49312.1>.
- Frank, T.D.; Thomas, S.G.; Fielding, C.R. On using carbon and oxygen isotope data from glendonites as paleoenvironmental proxies: A case study from the Permian system of eastern Australia. *J. Sediment. Res.* **2008**, *78*, 713–723. <https://doi.org/10.2110/jsr.2008.081>.
- Kassen, H.; Dmitrenko, I. The TRANSDRIFT II Expedition to the Laptev Sea Reports on Polar research, Laptev Sea Systems Expedition in Beretten. *Polarforsch* **1995**, *182*, 93. ISSN 01 76-5027.
- Kennedy, G.L., Hopkins, D.M., Pickthorn, W.J. *Ikaite, the Glendonite Precursor, in Estuarine Sediments at Barrow, Arctic Alaska, Abstracts with Programs*, Geological Society of America: Boulder, CO, USA, 1987.
- Schultz, B.P.; Hugget, J.M.; Kenndy, G.L.; Burger, P.; Friis, H.; Jensen, A.M.; Kanstrup, M.; Bernasconi, S.M.; Thibault, N.; Ullmann, C.V.; et al. Petrography and geochemical analysis of Arctic ikaite pseudomorphs from Utqiagvik (Barrow), Alaska. *Nor. J. Geol.* **2023**, *103*, 202303. <https://doi.org/10.17850/njg103-1-3>.
- Bohrmann, G.; Aromokeye, A.D.; Bihler, V.; Dehning, K.; Dohrmann, I.; Gentz, T.; Grahs, M.; Hogg, O.; Hüttich, D.; Kasten, S.; et al. R/V METEOR Cruise Report M134, Emissions of Free Gas From Cross-shelf Troughs of South Georgia: Distribution, Quantification, and Sources for Methane Ebullition Sites in Sub-Antarctic Waters, Port Stanley (Falkland Islands)—Punta Arenas (Chile), 16 January–18 February 2017. Berichte, MARUM—Zentrum für Marine Umweltwissenschaften, Fachbereich Geowissenschaften, Universität Bremen. 2017; Volume 317; pp. 1–220. Available online: <https://media.suub.uni-bremen.de/handle/elib/3351> (accessed on 1 June 2023).
- Wefer, G.; Strasser, M.; Besuden, E.; Büttner, H.; Diekamp, V.; Dinten, D.; dos SantosFerreira, C.; Fink, H.; Franke, P.; Fujiwara, T.; et al. Report and Preliminary Results of R/V SONNE Cruise SO219A, Tohoku-Oki-Earthquake—Japan Trench, Yokohama—

- Yokohama, 8 March 2012–6 April 2012, pp. 1–83. Available online: <http://publications.marum.de/id/eprint/2362> (accessed on 1 June 2023).
27. Ullmann, C.V.; Boyle, R.; Duarte, L.; Hesselbo, S.; Kasemann, S.; Klein, T.; Lenton, T.; Piazza, V.; Aberhan, M. Warm afterglow from the Toarcian Oceanic Anoxic Event drives the success of deep-adapted brachiopods. *Sci. Rep.* **2020**, *10*, 1–11. <https://doi.org/10.1038/s41598-020-63487-6>
 28. Schultz, B.P.; Vickers, M.L.; Huggett, J.; Madsen, H.; Heilmann-Clausen, C.; Friis, H.; Suess, E. Palaeogene glendonites from Denmark. *Bull. Geol. Soc. Den.* **2020**, *68*, 23–35. <https://doi.org/10.37570/bgds-2020-68-03-rev>.
 29. Vickers, M.; Watkinson, M.; Price, G.D.; Jerrett, R. An improved model for the ikaite-glendonite transformation: evidence from the Lower Cretaceous of Spitsbergen, Svalbard. *Nor. J. Geol.* **2018**, *98*, 15.
 30. Scheller, E.L.; Ingalls, M.; Eiler, J.; Grotzinger, J.; Ryb, U. The mechanisms and stable isotope effects of transforming hydrated carbonate into calcite pseudomorphs. *Geochim. Et Cosmochim. Acta* **2023**, Available online: <https://doi.org/10.1016/j.gca.2023.04.025> (accessed on 1 May 2023).
 31. Tollefsen, E.; Stockmann, G.; Skelton, A.; Mörtz, C.M.; Dupraz, C.; Sturkell, E. Chemical controls on ikaite formation. *Mineral. Mag.* **2018**, *82*, 1–22. <https://doi.org/10.1180/mgm.2018.110>.
 32. Hiruta, A.; Matsumoto, R. Geochemical comparison of ikaite and methane-derived authigenic carbonates recovered from Echigo Bank in the Sea of Japan. *Mar. Geol.* **2022**, *443*, 106672. <https://doi.org/10.1016/j.margeo.2021.106672>
 33. Whiticar, M.J.; Suess, E.; Wefer, G.; Müller, P.J. Calcium Carbonate Hexahydrate (Ikaite): History of Mineral Formation as Recorded by Stable Isotopes. *Miner.* **2022**, *12*, 1627. <https://doi.org/10.3390/min12121627>
 34. Pedersen, G.K.; Buchardt, B. The calcareous concretions (cementsten) in the Fur Formation (Paleogene, Denmark). Isotopic evidence of early diagenetic growth. *Bull. Soc. Geol. Den.* **1996**, *43*, 78–86.
 35. Stokke, E.W.; Jones, M.T.; Tierney, J.E.; Svensen, H.H.; Whiteside, J.H. Temperature changes across the Paleocene-Eocene Thermal Maximum—A new high-resolution TEX86 temperature record from the Eastern North Sea Basin. *Earth Planet. Sci. Lett.* **2020**, *544*, 116338. <https://doi.org/10.1016/j.epsl.2020.116338>.
 36. Jones, M.T.; Percival, L.M.E.; Stokke, E.W.; Frieling, J.; Mather, T.A.; Riber, L.; Schubert, B.A.; Schultz, B.; Tegner, C.; Planke, S. et al. Mercury anomalies across the Palaeocene-Eocene Thermal Maximum. *Clim. Past* **2019**, *15*, 217–236. <https://doi.org/10.5194/cp-15-217-2019>
 37. Vickers, M.L.; Lengger, S.K.; Bernasconi, S.M.; Thibault, N.; Schultz, B.P.; Fernandez, A.; Ullmann, C.V.; McCormack, P.; Bjerrum, C.J.; Rasmussen, J.A. Cold spells in the Nordic Seas during the early Eocene Greenhouse. *Nat. Commun.* **2020**, *11*, 1–12.
 38. McNamara M.E., Briggs D.E.G.; Orr P.J.; Field, D.J., Wang Z. Experimental maturation of feathers: implications for reconstructions of fossil feather colour. *Biol Lett.* **2013**, *9*. <http://dx.doi.org/10.1098/rsbl.2013.0184>.
 39. Lindgren, J.; Nilsson, D.; Sjövall, P.; Jarenmark, M.; Ito, S.; Wakamatsu, K.; Kear, B.P.; Schultz, B.P.; Sylvestersen, R.L.; Madsen, H. et al. Fossil insect eyes shed light on trilobite optics and the arthropod pigment screen. *Nat.* **2019**, *573*, 122–125, <https://doi.org/10.1038/s41586-019-1473-z>.
 40. Pedersen, G.K.; Pedersen, S.A.S.; Bonde, N.; Heilmann-Clausen, C.; Larsen, L.M.; Lindow, B.; Madsen, H.; Pedersen, A.K.; Rust, J., Schultz, B.P.; et al. Molerområdets geologi - sedimenter, fossiler, askelag og glacialtektonik. *Geol. Tidsskr.*, **2011**, 41–135.
 41. Jones, M.T.; Stokke, E.W.; Rooney, A.D.; Frieling, J.; Pogge von Strandmann, P.A.E.; Wilson, D.J.; Svensen, H.H.; Planke, S.; Adatte, T.; Thibault, N.; et al. Tracing North Atlantic volcanism and seaway connectivity across the Paleocene–Eocene Thermal Maximum (PETM), Available online: <https://egusphere.copernicus.org/preprints/2023/egusphere-2023-36/> (Accessed on 16 January 2023)
 42. Stokke, E.W.; Jones, M.T.; Riber, L.; Haflidason, H.; Midtkandal, I.; Schultz, B.P.; Svensen, H.H.. Rapid and sustained environmental responses to global warming: the Paleocene–Eocene Thermal Maximum in the eastern North Sea. *Clim. Past* **2021**, *17*, 1–25. <https://doi.org/10.5194/cp-17-1-2021>.
 43. Lindgren, J.; Uvdal, P.; Sjövall, P.; Nilsson, D.E.; Schultz, B.P.; Theil, V. Molecular preservation of the pigment melamin in fossil melanosomes. *Nat. Commun.* **2012**, *3*, 824. <https://doi.org/10.1038/ncomms1819>.
 44. Lindgren, J.; Sjövall, P.; Carney, R.M.; Uvdal, P.; Gren, J.A.; Dyke, G.; Schultz, B.P.; Shawkey, M.D.; Barnes K.R.; Polcyn, M.J. Skin pigmentation provides evidence of convergent melanism in extinct marine reptiles. *Nat.* **2014**, *506*, 484–488. <https://doi.org/10.1038/nature12899>.
 45. Heingård, M.; Sjövall, P.; Sylvestersen, R.L.; Schultz, B.P.; Lindgren, J. Crypsis in the pelagic realm: Evidence from exceptionally preserved fossil fish larvae from the Eocene Stolleklint Clay Den. *Palaeontol.* **2021**, *64*, 805–815. <https://doi.org/10.1111/pala.12574>.
 46. Heingård, M.; Sjövall, P.; Schultz, B.P.; Sylvestersen, R.L.; Lindgren, J. Preservation and Taphonomy of Fossil Insects from the Earliest Eocene of Denmark. *Biol.* **2022**, *11*, 395. <https://doi.org/10.3390/biology11030395>.
 47. Lázár, A.; Molnár, Z.; Demény, A.; Kótai, L.; Trif, L.; Béres, K.; Bódis, E.; Bortel, G.; Aradi, L.; Karlik, M. et al. Insights into the amorphous calcium carbonate (ACC) → ikaite → calcite transformations. *Cryst. Eng. Comm.* **2022**, *25*. <https://doi.org/10.1039/D2CE01444K>.

48. Németh, P. Diffraction Features from (1014) Calcite Twins Mimicking Crystallographic Ordering. *Miner.* **2021**, *11*, 720. <https://doi.org/10.3390/min11070720>.
49. Raven, M.J.; Dickson, J.A.D., Fir-tree zoning: an indicator of pulsed crystallization in calcite cement crystals. *Sediment. Geol.*, **1989**, *65*, 249–259, [https://doi.org/10.1016/0037-0738\(89\)90027-4](https://doi.org/10.1016/0037-0738(89)90027-4).

Disclaimer/Publisher's Note: The statements, opinions and data contained in all publications are solely those of the individual author(s) and contributor(s) and not of MDPI and/or the editor(s). MDPI and/or the editor(s) disclaim responsibility for any injury to people or property resulting from any ideas, methods, instructions or products referred to in the content.